American Journal of Chemistry 2026, 16(2): 31-39
DOI: 10.5923/j.chemistry.20261602.01

# Detection of Oxacillin in Matrices Using Boron-Doped Diamond Electrode: A Voltammetry Study

**Kone Souleymane[1,*], Kone Siriki[2], Kimou Kouakou Jocelin[3], Koffi Konan Sylvestre[1], Lassine Ouattara[1]**

[1]Laboratory of Constitution and Reaction of Matter, UFR SSMT, Felix Houphouet Boigny University, Abidjan, Ivory Coast
[2]Department of Science and Technology, Alassane Ouattara University, Bouake, Ivory Coast
[3]Institute for Research on New Energies, Nangui Abrogoua University, Ivory Coast

**Abstract** The release into the environment of persistent organic pollutants, such as oxacillin, is a source of environmental concern. The objective of this study is to propose an effective and less expensive method for determining the concentrations of this pollutant in the environment. In this work the detection and oxacillin were performed using cyclic voltammetry and square-wave voltammetry (SWV). The anode used is a boron-doped diamond electrode (BDD). The characterization of the BDD electrode surface by scanning electron microscopy and by the electrochemical method (cyclic voltammetry) showed the high quality of the electrode and its ability to quantify oxacillin. SWV method allowed to obtain the calibration curve for oxacillin concentrations ranging from 4 µM to 76.15 µM with detection limit of 1,705 µM in 0,1 M $K_2SO_4$. The suggested method was effectively implemented assess these analytes in real matrices such as vegetable juice with recovery rates ranging from 81.54% to 100.32%. Oxacillin was detected in an ionic media, and it found that interference was negligible during detection.

**Keywords** Oxacillin, Detection, Square-wave voltammetry, Boron-doped diamond

## 1. Introduction

Emergencing pollutants, including pharmaceuticals, represent worldwide public health concerns for several decades, mainly due to the constant emergence of new types of pharmaceutic products [1,2]. The considerable presence and accumulation of these substances in the aquatic environment is mainly due to the release of industrial effluents, notably pharmaceutical effluents, along with domestic and hospital wastewater [3,4]. This leads to the development of antibiotic -resistant bacteria, rendering these products ineffective in treatment infections [5]. Among the pharmaceutical products is oxacillin (OXA), a substance in the penicillin family used widely in the treatment of infections [6]. Oxacillin, a semisynthetic antibiotic from the β-lactam class, is a molecule that is not biodegradable [7] and can be metabolized or not by the human body. It is almost entirely excreted in the faeces or urine after administration. Its degradation by conventional wastewater treatment is incomplete, so OXA enters our waterways [8] at concentration levels reaching very large amounts and more precisely in surface water [9,10]. Their presence in nature perturbs aquatic ecosystems.

* Corresponding author:
souleymanekone7351@gmail.com (Kone Souleymane)
Received: May 2, 2026; Accepted: May 23, 2026; Published: May 29, 2026
Published online at http://journal.sapub.org/chemistry

Unfortunately, few studies have been conducted on the detection of oxacillin in the environment, and the most commonly used methods for detecting and quantifying this pharmaceutical product are mass spectrometry coupled with direct injection liquid chromatography (HPLC) and capillary electrophoresis (CE) [10]. These approaches require complex equipment and sufficient financial resources. Hence, the electrochemical detection of this pharmaceutical compound is of interest, due to the fact that this method allows for the detection of low concentrations while ensuring high sensitivity and selectivity. Several electrochemical sensors have proven effective in the detection and quantification of pharmaceuticals, notably the platinum electrode [11,12], the carbon electrode [13,14], and boron-doped diamond (BDD) [15,16], using analytical methods such as cyclic voltammetry (CV), square-wave voltammetry (SWV), or differential pulse voltammetry (DPV). The BDD electrode is an electrode with interesting electrochemical properties, including high thermal conductivity, high hardness, very high stability, chemical inertness, and a wide electrochemical potential window in both aqueous and non-aqueous media [17]. Using a BDD electrode allowed us to find a very good detection limit [18-20].

In this study, using a BDD electrode, the aim is to detect OXA in a synthetic solution (0.1 M $K_2SO_4$) and to prove the effectiveness of this approach by detecting this substance in a real media such as vegetable juices.

# 2. Materials and Methods

### 2.1 Electrode Preparation

Boron doped diamond (BDD) electrodes were fabricated by hot-filament chemical vapor deposition (HF-CVD) on low resistivity (1-3 mΩ.cm) p-Si wafers. The wafers, which came from siltronix, were each 10 cm in diameter and a thickness of 0.5 mm). Trimethylboron was then introduced into the process gas consisting of 1 % $CH_4$ in $H_2$ to allow boron doping. Film growth was carried out at a rate of 0.24 $\mu m.h^{-1}$. The film thickness was approximately 1 µm which made it uniformly coated on the whole surface of the wafer.

### 2.2. Measurement Methods

An Autolab PGStat 20 (Ecochemie) linked to a potentiostat equipped with USB electrochemical interface was used to conduct voltammetric measurements on the BDD electrode in a three-electrode electrochemical cell: a working electrode, a counter electrode (CE), a reference electrode (RE). A platinum wire served as the counter electrode. A saturated calomel electrode (SCE) was used as the reference electrode. The working electrode was a BDD electrode with a geometrical contact area of 1 $cm^2$. To overcome the potential ohmic drop, the reference electrode was placed in a luggin capillary close to working electrode. The equipment is connected a data processing and storage computer equipped with GPES 4 software to start and record the voltammograms.

Prior to the experiments, the BDD electrode was electrochemically pretreated in a 0.5 M $H_2SO_4$ solution. For this pre-treatment, an anodic pre-treatment (+2V, 15 s) is followed by a cathodic pre-treatment (-2 V, 90 s). In this way, the BDD surface was first cleaned of all impurities and then rendered mainly hydrogen [21].

### 2.3. Chemicals

Oxacillin [(2S,5R,6R)-5-hydroxy-3,3-dimethyl-6-{[(5-methyl-3-phenyl-1,2-oxazol-4-yl) carbonyl] amino}-4-thia-1-azabicyclo [3.2.0] heptane-2-carboxylic acid] with the empirical formula $C_{19}H_{21}N_3O_5S$ was purchased from pharmacies in Abidjan. It was prepared by dissolving an accurate mass of the drug in an appropriate solution of 0.1 M of potassium sulfate $K_2SO_4$ (Panreac) used for the supporting electrolyte. Ultrapure distilled water was used to prepare the supporting electrolyte.

Following a specific procedure, the vegetable juices employed in this project were obtained. Initially, each of these market-purchased vegetables was thoroughly cleaned with tap water and then with distilled water. After that, each vegetable was pulverized one at a time in a spotless blender using a precisely measured amount of 0.1 M of sodium sulfate $K_2SO_4$. After that, the juice was repeatedly filtered using regular filter paper (Filter-LaB) to produce a homogenous juice. The 100 ml stock of juice utilized as a supporting electrolyte was finally obtained by dissolving 1 ml of this filtrate in a volumetric flask filled with 0.1 M $K_2SO_4$.

The β-lactam ring of the oxacillin molecule is often susceptible to hydrolytic and photolytic degradation. Therefore, working solutions were prepared on the day of use, stored away from direct light, and discarded after 24 hours, so that the recorded response corresponded to intact oxacillin and was not distorted, if possible, by other products.

# 3. Results and Discussion

### 3.1. Physical Characterization of the Electrode

The scanning electron microscope (SEM) image of the BBD electrode is displayed in **Figure 1**. The image shows randomly oriented crystals measuring a few micrometers (between 0.3 and 0.6 µm). These crystals, which have different crystal faces, are strongly bonded to one another. This image indicates that BDD has a polycrystalline structure [22]. Indeed, in chemical vapor deposition (CVD): diamond crystallites develop independently from numerous nucleation sites on the silicon wafer, each growing in its own crystallographic direction until reaching its neighbors. The final film thus appears as a mosaic of grains, bounded by crystalline faces and visible grain boundaries, rather than as a continuous monocrystalline lattice. Furthermore, some crystal faces are darker than others. This contrast is thought to be due to a higher boron content [23].

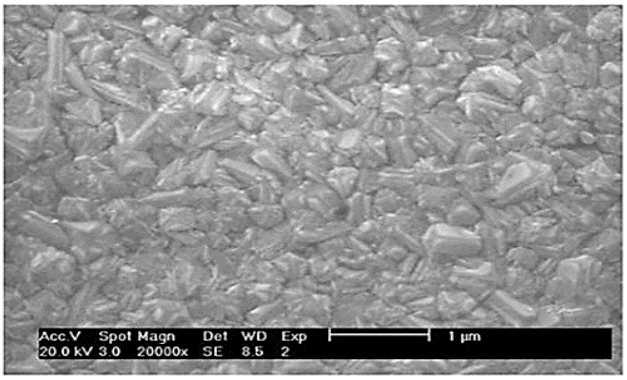


**Figure 1.** SEM image of BDD electrode surface

### 3.2. Electrochemical Characterization of the Electrode

The electrochemical characterization of the BDD electrode was performed in a 0.1 M $K_2SO_4$ over a potential range of –1.5 V/SCE to 2.2 V/SCE. The measurements were performed under a potential scan rate of 50 mV/s The results are shown in **Figure 2**. The voltammogram obtained shows three regions.

At a potential of – 0.9 V/SCE, a rapid increase in current density in absolute value, corresponds to the dihydrogen release domain. At potentials higher than 1.48 V/SCE, a rapid increase in current density in the anodic region is observed reflecting the oxygen evolution reaction. The region bounded by the onset of dihydrogen evolution and that of oxygen evolution is called the electroactivity domain of the supporting electrolyte with a potential window $\Delta E$ =

2.38 V. We note in this area the absence of electrochemical reaction, as evidenced by a current that is quasi- null. Indeed, we observe that no modification (peak characteristic of oxide layer formation) occurs on the electrode surface in this electrolyte solution, indicating the inert nature and thus the stability of the BDD regarding acid corrosion.

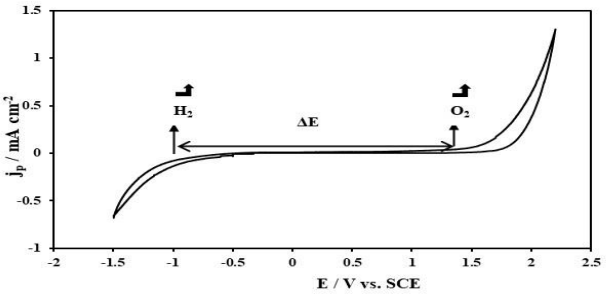


**Figure 2.** Voltammetric curve of BDD in $K_2SO_4$ (0.1M) at 50 mV/s

### 3.3. Electrochemical Behavior of the Electrode

**Figure 3A** shows the voltammetric measurements in the presence of various concentrations of OXA in $K_2SO_4$ (0.1 M). The current density of the oxidation peaks increases with the OXA concentration. After adding OXA, an anodic peak appears at 1.6 V/SCE. This indicates oxidation of OXA on the BDD [24]. The curve of the oxidation peak current versus the OXA concentration are shown in **Figure 3B**. The straight line obtained with a coefficient of determination ($R^2$ = 0,9949) close to 1, indicates that OXA present in the medium is responsible for the changes observed in the voltammogram. Oxidation peak is related to the OXA oxidation. The absence of peaks in the reverse direction would imply irreversibility of the process. These results suggest that the BDD electrode could be useful for the quantitative determination of OXA.

### 3.4. Square-Wave Voltammetries

#### 3.4.1. Measurement Conditions

In the interest of more efficient voltammetric detection of the pharmaceutical substance, certain VOC parameters were optimized. These parameters include frequency, amplitude, and potential step. The optimization was intended to improve sensitivity, signal resolution, and measurement reproducibility.

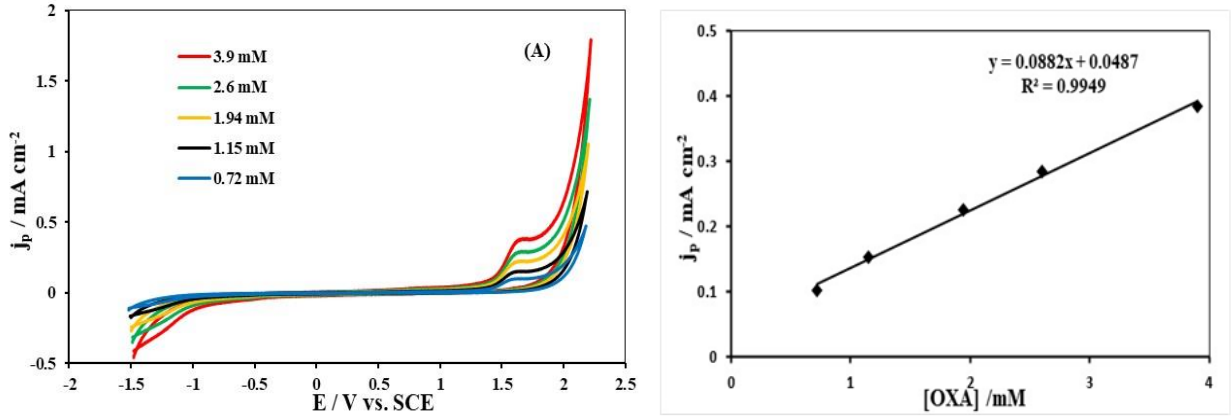


**Figure 3.** (A) Cyclic voltammogram of different OXA concentrations in $K_2SO_4$ (0.1M) at 50 mV/s; (B): plot of $J_P$ = f ([OXA]

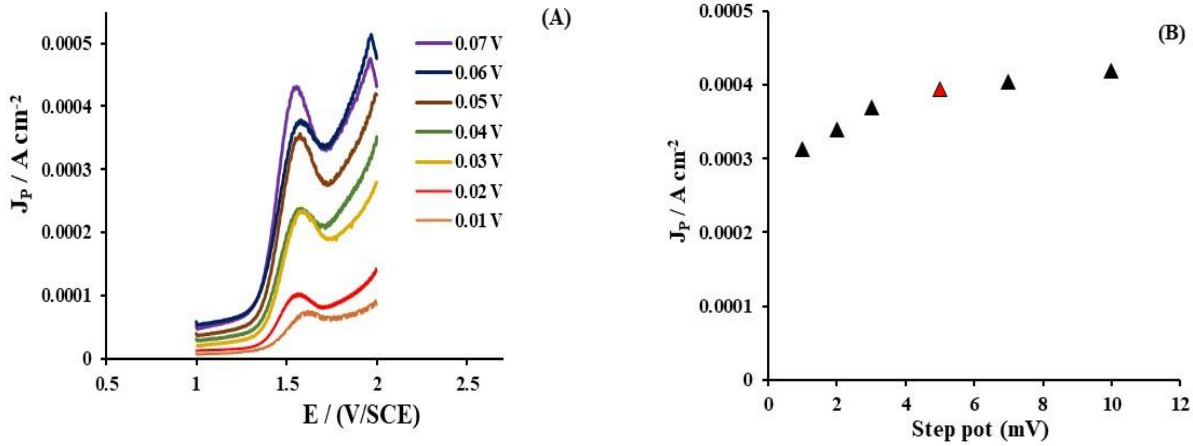


**Figure 4.** (A) Square-wave voltammograms as a function of amplitude; (B) Variations in the peak oxidation current densities as a function of potential step; 0.5 mM OXA in 0.1 M $K_2SO_4$

To determine the frequency, square-wave voltammetric (SWV) analyses were performed by varying the frequency (f) in 5 Hz increments from 15 Hz to 35 Hz. At 25 Hz, the voltammogram is smooth and clear, with a more distinct peak and less background noise. In contrast, the curves for the other frequencies were not sufficiently clear and smooth. These observations may have been due to interference between the system and the external environment. However, since the experiment was not conducted in a Faraday cage to limit such interference, the optimal frequency selected is 25 Hz. Using this frequency, each parameter was then varied while keeping the others constant. The obtained results are shown in the **Figure 4**.

The effect of amplitude (AM) was investigated. An increase in peak oxidation current with amplitude was observed (**Figure 4A**). Furthermore, we also observe a shift of the peak potentials to the left and a slightly broader shape of the voltammograms below an amplitude of 0.05 V. Above 0.05 V, starting at a potential of 0.06 V/SCE, the shape of the voltammogram changes. To avoid these risks of selectivity in the oxacillin oxidation peak, it is preferable not to choose amplitude values that are too high. In this regard, 0.05 V (50 mV) was used as the amplitude.

For the remainder of this study. The amplitude and frequency were adjusted to 50 mV and 25 Hz, respectively. The measurements were carried out in the potential range from 1 mV/ECS to 10 mV/ECS. In **Figure 4B**, an increase in peak currents with the potential step (ΔEstep) is noted up to 5 mV, where a small plateau is apparent, indicating saturation of the electrode surface at this value. Thus, the value of 5 mV was chosen as the potential step in this analytical method.

### 3.4.2. Detection and Quantification of Oxacillin by SWV Method

In order to validate this analysis method for determining OXA in pharmaceutical and environmental applications, OXA signals at various concentrations were recorded on the BDD electrode in potassium sulfate medium (0,1 M $K_2SO_4$). **Figure 5A** presents recorded voltammetric response curves of the oxidation peaks for each OXA concentration ranging from 0 µM to 76.15 µM. These voltammograms were obtained under optimal conditions: AM = 50 mV/SCE, f = 25 Hz, and ΔEstep = 5 mV/ECS. The oxidation peaks for each OXA concentration within the selected concentration range are observed for a potential of around 1.6 V/ECS. This relatively positive oxidation potential corresponds to an electron transfer involving the oxidizable group of the oxacillin molecule, and its detection for analytical purposes is facilitated by the exceptionally wide anodic window of the DDB electrode (ΔE = 2.38 V, Section 3.2), on which solvent discharge is strongly repelled. On conventional electrodes such as platinum or glassy carbon, this peak would instead be masked by oxygen evolution. It is also apparent that peak current density increases with OXA concentration.

The dependence of the peak oxidation current density and the OXA concentration in the electrolyte allows the calibration curve to be plotted over the concentration range from 4 µM to 76.15 µM. The curve obtained is a straight line with a determination coefficient $R^2 = 0.999$, which is close to 1 follows the **Equation (1)**.

$$j_p = 2*10^6\ C + 0.00001 \quad (1)$$

This result suggests good linearity of the method for the selected concentration range. The limits of detection (LOD) and quantification (LOQ) were determined based on the expressions in **Equations (2)** and (**3)** and experimental measurements. Their respective values are 1.705 µM and 5.683 µM.

$$LOD = 3*SD / b \quad (2)$$

$$LOQ = 10*SD / b \quad (3)$$

Where SD is the standard deviation of the current density signals and b is the slope of the method calibration curve.

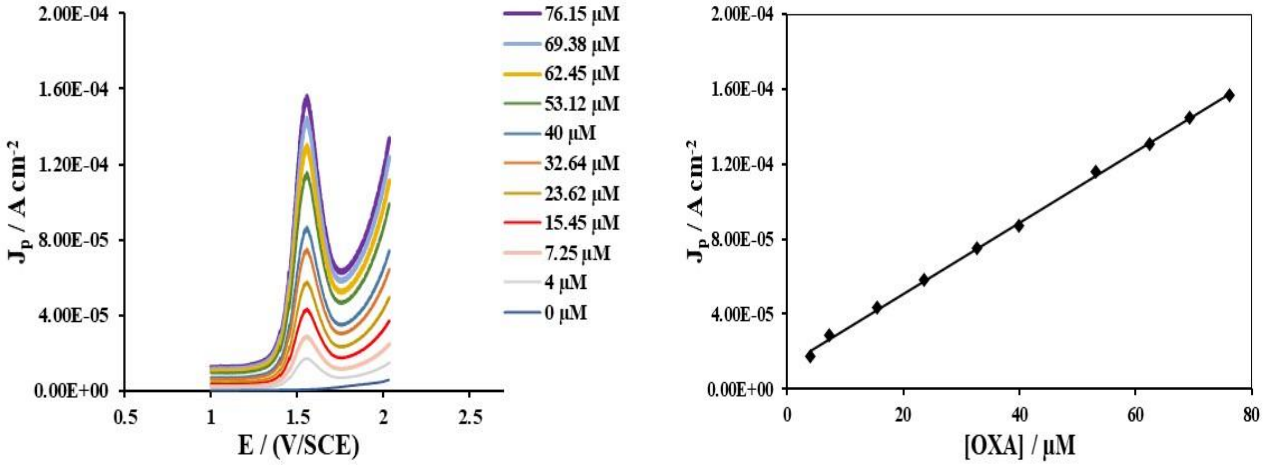


**Figure 5.** (A) Square-wave voltammetries (SWV) of OXA (0 µM to 76.15 µM); (B) $J_p$ curve versus OXA concentration

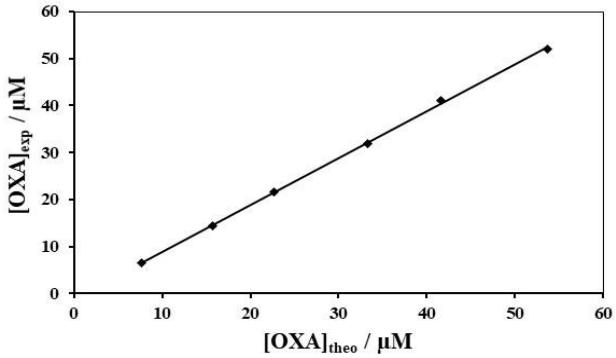


**Figure 6.** Plot of experimental concentration versus theoretical concentration

For determining the recovery rate, six (6) samples containing different concentrations of oxacillin ([OXA]theo) were used. For each sample, three independent measurement runs were performed using metered additions. These concentrations were calculated after the successive addition of well-defined volumes of the OXA stock solution prepared in the measurement cell. The results obtained are shown in **Table 1**. Using the calibration curve obtained from **Equation (1)**, the experimental concentration ([OXA]exp) was estimated for each of the different theoretical concentrations ([OXA]theo) of oxacillin used. The plot of the experimental concentration as a function of the theoretical oxacillin concentration is shown in **Figure 6**. The linear curve obtained has an $R^2$ value of 0.9996, which is very close to 1, from the **Equation (4)**:

$$[OXA]_{exp} = 1{,}0003\ [OXA]_{theo} - 1{,}1587 \qquad (4)$$

This straight line has a slope that is practically equal to 1, indicating a linear relationship between the experimental and theoretical concentrations of oxacillin and also proving the reliability of the square-wave voltammetric analytical method. The calculation of the oxacillin recover rate subsequently ranges from (84.89 ± 0.05) to (98.72 ± 0.74). These elevated rates indicate that this method can be used for the detection and quantification of oxacillin in media [25,26].

The wastewater sometimes contains several pharmaceutical organic compounds [27]. In this study, we will examine the possibility of detecting OXA in a more complex matrix containing both paracetamol (PCM) on the BDD electrode using square-wave voltammetry. Various studies have shown that oxidation peak of paracetamol appears around 0.6 V/SCE [28,29]. Thus, the voltammograms from this matrix were recorded under the optimized conditions obtained with OXA alone in a potassium sulfate (0.1 M $K_2SO_4$) medium. OXA and PCM were detected by simultaneously varying their concentrations (**Figure 7**). The VOC results show that the simultaneous detection of OXA and PCM, with two well-defined anodic peaks at potentials around 1.6 V and 0.6 V/SCE, respectively, is possible with good analyte selectivity.

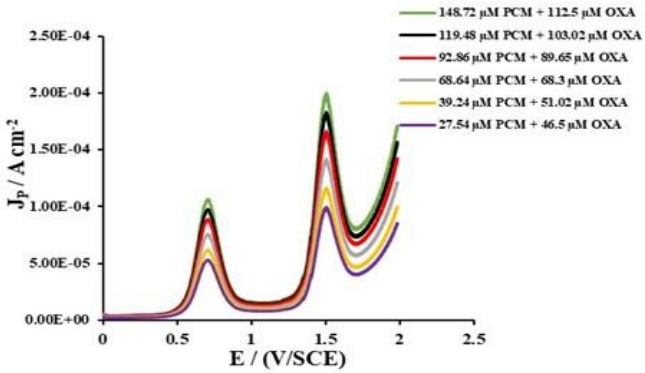


**Figure 7.** Square-wave voltammograms of BDD with different OXA and PCM concentrations

**Table 1.** Recovery rate of the method

| Sample number | Introduced concentration (µM) | Found concentration (µM) | Recovery rate ± SD |
|---|---|---|---|
| 1 | 7,72 | 6,56 | (84,89 ± 0,05) |
| 2 | 15,76 | 14,39 | (91,31 ± 0,09) |
| 3 | 22,65 | 21,62 | (95,4 ± 0,4) |
| 4 | 33,25 | 31,96 | (96,1 ± 0,5) |
| 5 | 41,54 | 41,01 | (98,7 ± 0,7) |
| 6 | 53,62 | 52,10 | (97,2 ± 0,9) |

**Table 2.** Influence inorganic ions on OXA detection

| Interfering Compounds | Concentration in mmol/L of added interferent | % Change in peak current density in SWV |
|---|---|---|
| ($2Na^+$; $SO_4^{2-}$) | 3.536 | -3.310 |
| | 7.205 | 1.263 |
| | 10.512 | 4.882 |
| (**2**$K^+$; $HPO_4^{2-}$) | 3.536 | -5.019 |
| | 7.205 | -2.863 |
| | 10.512 | -1.019 |
| ($K^+$; $NO_3^-$) | 3.536 | -0.392 |
| | 7.205 | 1.745 |
| | 10.512 | 3.117 |

3.4.3. Interferences Studies

Inorganic ions are widely present in the environment, and the effect of some of them on oxacillin detection was investigated. The interfering species of interest were potassium nitrate ($K^+$; $NO_3^-$), sodium sulfate ($2Na^+$; $SO_4^{2-}$), and potassium hydrogen phosphate ($2K^+$; $HPO_4^{\wedge}(2-)$). Thus, concentrations of each interfering compound (3.536, 7.205, and 10.512 mM) were added to $K_2SO_4$ (0.1 M) media containing 25 µM OXA. Based on the square wave voltammetric curves recorded, the peak current densities of OXA were determined for each concentration of the interfering species. The interference (X, in %) of each compound on the OXA signal is calculated using the formula (**Equation (5)**)

$$X = \left(\frac{J'}{J} \times 100\right) - 100 \quad (5)$$

Where J' is the peak density of the interfered signal of each drug product and J is that of the signal without interferents.

The results are reported in **Table 2**. The results suggest that certain ions, such as $K^+$, $Na^+$, $SO_4^{2--}$, $NO_3^-$ and $HPO_4^{2-}$ which are more concentrated than oxacillin, produce a negligible effect on the current density of the OXA oxidation peak in a 0.1 M $K_2SO_4$ media. For the OXA signal (SWV), the relative uncertainty registered is approximately ±5%, which corresponds to the acceptable tolerance limit for a maximum concentration of added substances or interfering substances [30]. It is therefore significant that there was no interference from the ions mentioned above on the oxidation of OXA in a neutral medium. Thus, this pharmaceutical organic compound can be detected and quantified by a BDD electrode even in charged ion media such as wastewater using SWV.

3.4.4. Application to Detection of OXA

To assess the applicability of the proposed method, OXA was detected in complex media such as cucumber, tomato, and cabbage-based juices. These complex media were used as electrolyte carriers as described in the experimental section. The OXA content varied by adding measured amounts to each support. The voltammetric curves obtained from this analysis, as well as the relationship the peak oxidation current density as a function OXA concentration, are plotted in **Figure 8**. These different figures reveal that the voltammograms exhibit the same peak oxidation potential (1.6 V/SCE), and the peak current densities are of the same order of quantity depending on the amount of OXA added to the measurement cell. Indeed, in each medium, the peak currents increase with the OXA concentration, which reflects the direct proportionality between the diffusion-controlled faradic current and the amount of electroactive oxacillin reaching the electrode surface. The calibration curves provide good linearity ($R^2$ close to 1). This information demonstrates that the method used is selective and also that OXA can be analyzed equally well in a potassium sulfate media as in complex media. The limits of detection and quantification in the concentration range selected, as obtained for the various matrices, are indicated in **Table 3**. They are all of the same size order. The proposed electrochemical method allows for the detection of oxacillin.

**Table 3.** Limits of detection and quantification

| Electrolyte | LOD (µM) | LOQ (µM) |
|---|---|---|
| Cucumber juice | 4.121 | 13.737 |
| Tomato juice | 5.301 | 17.672 |
| Cabbage-based juice | 3.665 | 12.216 |

To further ensure the accuracy of this method, recovery rates were estimated for each sample (**Table 4**). The recovery rates for OXA were found to be quite high in the various carrier electrolytes. This demonstrates the high accuracy of the method and the absence of a significant matrix effect: thanks to the low and stable baseline current, the wide potential window, and the low adsorption of organic species on the BDD surface, the oxidation signal of oxacillin is neither attenuated nor distorted by the composition of the vegetable juices. These values, ranging generally from 81.54% to 100.32%, thus attest to the applicability of this method for the detection of oxacillin in different matrices [31].

**Table 4.** Recovery rates for OXA detection in cucumber, tomato, and cabbage-based juices under the same detection conditions

| Electrolyte | Introduced Concentration (µM) | Found Concentration (µM) | Recovery rate ± SD |
|---|---|---|---|
| Cucumber juice | 9.98 | 8.97 | **(89.9 ± 0.3)** |
| | 14.84 | 13.73 | **(92.5 ± 0.2)** |
| | 28.95 | 27.25 | **(94.11 ± 0.07)** |
| | 40.86 | 40.92 | **(100.1 ± 0.6)** |
| | 55.87 | 54.38 | **(97.3 ± 0.2)** |
| Tomato juice | 9.98 | 8.15 | **(81.5 ± 0.3)** |
| | 14.84 | 14.08 | **(94.84 ± 0.09)** |
| | 28.95 | 29.05 | **(100.3 ± 0.7)** |
| | 40.86 | 39.48 | **(96.6 ± 0.1)** |
| | 55.87 | 55.08 | **(98.5 ± 0.4)** |
| Cabbage-based juice | 9.98 | 8.54 | **(85.6 ± 0.1)** |
| | 14.84 | 13.94 | **(93.9 ± 0.2)** |
| | 28.95 | 27.42 | **(94.6 ± 0.4)** |
| | 40.86 | 39.88 | **(97.60 ± 0.02)** |
| | 55.87 | 55.48 | **(99.2 ± 0.9)** |

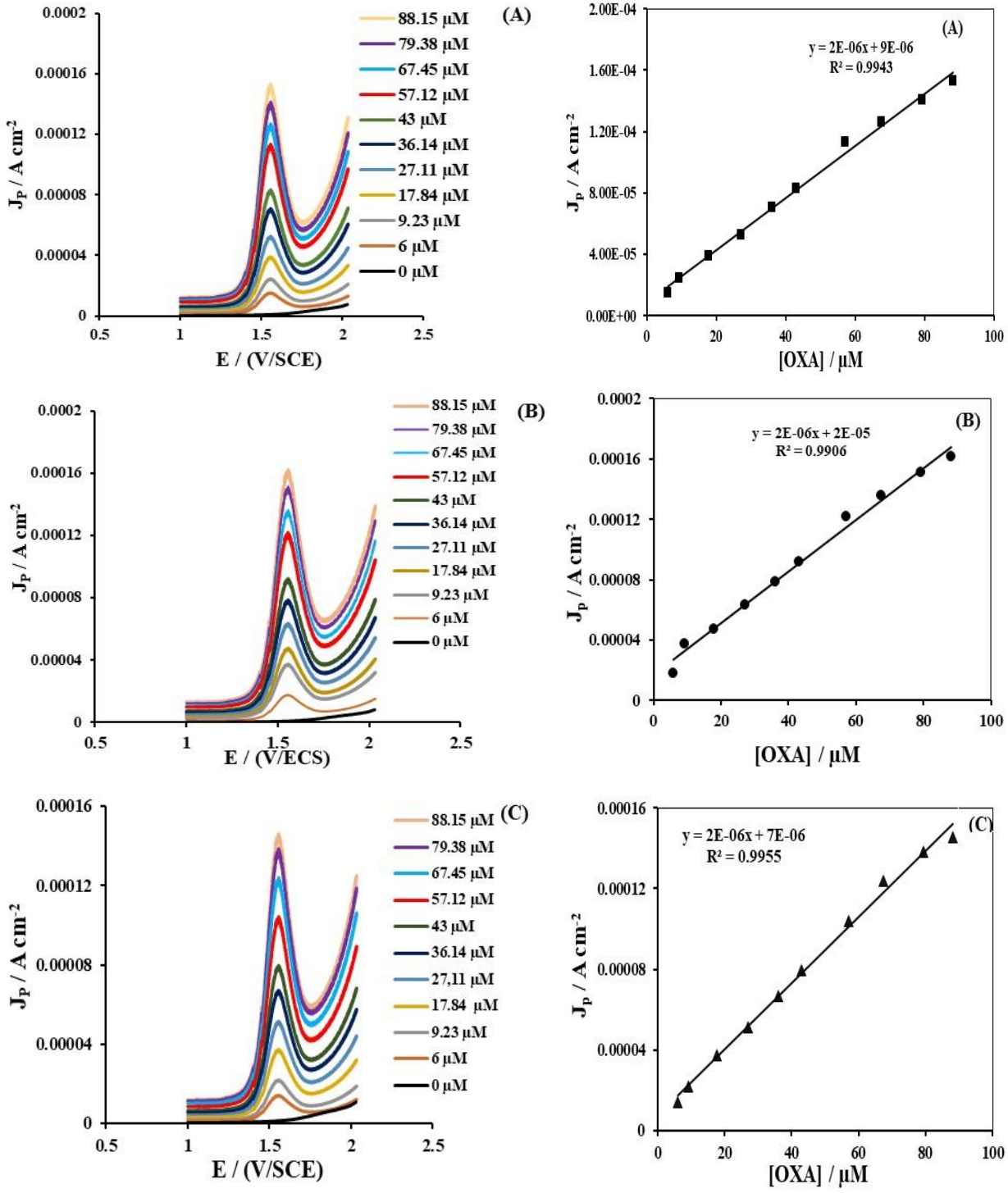


**Figure 8.** Square-wave voltammograms on the BDD electrode of different OXA concentrations in (A) cucumber juice, (B) tomato juice, and (C) cabbage-based juice, along with their calibration curves

## 4. Conclusions

The work carried out proves that boron-doped diamond is appropriate for the individual voltammetric detection of OXA, even in the presence of other organic and inorganic molecules. The data analysis indicates that square-wave voltammetry (SWV) can serve as a valuable tool for the quantitative and qualitative identification of the pharmaceutical compound alone or in combination, as commonly found in pharmaceutical formulations, wastewater, or potentially in certain fruit and vegetable juices. The high sensitivity of the electrode, primarily attributable to its excellent physicochemical properties, allowed us to obtain clearly defined, distinct oxidation peaks in SWV. The high recovery rates achieved

in various complex environments attest to the practical analytical utility of the sensor and the effectiveness of the method employed.

## ACKNOWLEDGEMENTS

We are thankful to the Swiss National Funds for its financial support. They funded the project (IZ01Z0_146919) which durability helped this work to be undertaken.

## Conflicts of Interest

The authors declare no conflicts of interest.

## REFERENCES

[1] Kimou, K. J., Kambiré, O., Koffi, K. S., Kouadio K. E., Koné, S., and Ouattara, L. (2021). Electrooxidation of Iohexol in Its Commercial Formulation Omnipaque on Boron Doped Diamond Electrode. International Research Journal of Pure & Applied Chemistry, 22 (11), 29-41. https://doi.org/10.9734/IRJPAC/2021/v22i1130444.

[2] Bilal, M., Ashraf, S. S., Barceló, D., and Iqbal, H. M. N. (2019). Biocatalytic degradation/redefining "removal" fate of pharmaceutically active compounds and antibiotics in the aquatic environment. Science of The Total Environment, 691, 1190-1211. https://doi.org/10.1016/j.scitotenv.2019.07.224.

[3] Lei, K., Zhu, Y., Chen, W., Pan, H. Y., Cao, Y. X., Zhang, X., and Ouyang, W. (2019). Spatial and seasonal variations of antibiotics in river waters in the Haihe River catchment in China and ecotoxicological risk assessment. Environment International, 130, 104919. https://doi.org/10.1016/j.envint.2019.104919.

[4] Rasheed, T., Bilal, M., Nabeel, F., Adeel, M., and Iqbal, H. M. N. (2019). Environmentally related contaminants of high concern: Potential sources and analytical modalities for detection, quantification, and treatment. Environment International, 122, 52-66. https://doi.org/10.1016/j.envint.2018.11.038.

[5] Sadia, S. P., Kambiré, O., Gnamba, C. Q-M., Pohan, L. A. G., Berté, M., and Ouattara, L. (2021). Mineralization of Wastewater from the Teaching Hospital of Treichville by A combination Biological Treatment and Advanced Oxidation Processes. Asian Journal of Chemical Sciences, 10(2), 1-10. https://doi.org/10.9734/AJOCS/2021/v10i219086.

[6] Hughes, D. W., Frei, Maxwell, C. R., Green, P. R. K., Patterson, J. E., Crawford, G. E., and Lewis, J. S. (2009). Continuous versus intermittent infusion of oxacillin for treatment of infective endocarditis caused by methicillin-susceptible Staphylococcus aureus. Antimicrob. Agents Chemother, 53, 2014–2019. https://doi.org/10.1128/aac.01232-08.

[7] Giraldo, A. L., Erazo-Erazo, E. D., Flórez-Acosta, O. A., Serna-Galvis, E. A., and Torres-Palma, R. A. (2015). Degradation of the antibiotic oxacillin in water by anodic oxidation with Ti/IrO2 anodes: Evaluation of degradation routes, organic by-products and effects of water matrix components. Chemical Engineering Journal, (2015), 279, 103–114. https://doi.org/10.1016/j.cej.2015.04.140.

[8] Pitout, J. D. D., Sanders, C. C., and Sanders, W. E. Jr. (1997). Antimicrobial resistance with focus on b-lactam resistance in gram-negative bacilli. American Journal of Medicine, 103, 51–59. https://doi.org/10.1016/S0002-9343(97)00044-2.

[9] Michael, I., Rizzo, L., McArdell, C. S., Manaia, C. M., Merlin, C., Schwartz, T., Dagot, C., and Fatta-Kassinos, D. (2013). Urban wastewater treatment plants as hotspots for the release of antibiotics in the environment: a review. Water Research, 47, 957–995. https://doi.org/10.1016/j.watres.2012.11.027.

[10] Cha, J. M., Yang, S., and Carlson, K. H. (2006). Trace determination of b-lactam antibiotics in surface water and urban wastewater using liquid chromatography combined with electrospray tandem mass spectrometry. Journal of Chromatography A, 1115, 46–57. https://doi.org/10.1016/j.chroma.2006.02.086.

[11] Riham, K. A., Engy, M. S., Hussein, M. F., and Rasha, M. E. N. (2021). Design and application of molecularly imprinted Polypyrrole/Platinum nanoparticles modified platinum sensor for the electrochemical detection of Vardenafil. Microchemical Journal, 171, 106771. https://doi.org/10.1016/j.microc.2021.106771.

[12] Alhazmi, H. A., Imran, M., Ahmed, S., Albratty, M., Makeen, H. A., Najmi, A., and Alam, M. S. (2023). Electrochemical detection of dopamine using $WSe_2$ microsheets modified platinum electrode. Physica Scripta, 98, 105006. https://doi.org/10.1088/1402-4896/acf07f.

[13] Lee, P. T., Thomson, J. E., Karina, A., Salter, C., Johnston, C., Davies, S. G., and Compton, R. G. (2015). Selective electrochemical determination of cysteine with a cyclotricathechylene modified carbon electrode. Analyst, 140, 236-242. https://doi.org/10.1039/C4AN01835D.

[14] Liu, Z., Liu, Y., He, L., Xue, Q., Zhao, and J., Pu, S. (2024). Advanced functional carbon electrode for ultra-sensitive detection of hexavalent chromium in water: performance, mechanism, and application. Chemical Engineering Journal, 500, 156799. https://doi.org/10.1016/j.cej.2024.156799.

[15] Karine, R. T., Luciano, C. A., Pablo, A. M., Anne, A. M., Dilton, M. P., Diego, P. R., Anderson C. O., Eduardo, M. R., Rodrigo, A. A. M., and Wallans, T. P. D. S. (2020). Electrochemical detection of 3,4-methylenedioxymethamphetamine (ecstasy) using a boron doped diamond electrode with differential pulse voltammetry: Simple and fast screening method for application in forensic analysis. Microchemical Journal, 157, 105088. https://doi.org/10.1016/j.microc.2020.105088.

[16] Feier, B., Gui, Ana., Cristea, Cecilia., and Săndulescu, R. (2017). Electrochemical determination of cephalosporins using a bare boron-doped diamond electrode. Analytica Chimica Acta, 976, 25-34. https://doi.org/10.1016/j.aca.2017.04.050.

[17] Gnamba, C. Q-M., Appia F. T. A., Loba, E. M. H., Sanogo I., Ouattara, L. (2015). Electrochemical oxidation of amoxicillin in its pharmaceutical formulation at boron doped diamond (BDD) electrode. J. Electrochem. Sci. Eng, 5(2), 129-143. https://doi.org/10.5599/jese.186.

[18] Moriyama, H., Ogata, G., Nashimoto, H., Sawamura, S., Furukawa, Y., Hibino, H., Kusuharab, H., and Einaga, Y. (2022). A rapid and simple electrochemical detection of the free drug concentration in human serum using boron-doped diamond electrodes. Analyst, 147, 4442-4449. https://doi.org/10.1039/D2AN01037B.

[19] Pei, J., Yu, X., Wei, S., Boukherroub, R., and Zhang, Y. (2021). Double-side effect of B/C ratio on BDD electrode detection for heavy metal ion in water. Science of The Total Environment, 771, 145430. https://doi.org/10.1016/j.scitotenv.2021.145430.

[20] Kramplová, Z., Ferancová, A., Maliar, I., and Purdešová, A. (2023). Tuneable properties of boron-doped diamond working electrodes and their advantages for the detection of pesticides. Journal of Electroanalytical Chemistry, 949, 117846. https://doi.org/10.1016/j.jelechem.2023.117846.

[21] Salazar-Banda, G. R., Andrade, L. S., Nascente, P. A. P., Pizani, P. S., Rocha-Filho, R. C., and Avaca, L. A. (2006). The changing electrochemical behaviour of boron-doped diamond surfaces with time after cathodic pre-treatments. Electrochim. Acta, 51, 4612-4619. https://doi.org/10.1016/j.electata.2005.12.039.

[22] May, P. W., and Zulkharnay, R. (2025). Diamond thin films: a twenty-first century material. Part 2: a new hope. Philosophical Transactions A, 383(2296), 20230382. https://doi.org/10. 1098/rsta.2023.0382.

[23] Spitsyn, B. V., Bouilov L. L., and Derjaguin, B. V. (1981). Vapor growth of diamond on diamond and other surfaces, Journal of Crystal Growth, 52, 219-226. https://doi.org/10. 1016/0022-0248(81)90197-4.

[24] Kone, S., Meledje, J. C., Kimou, K. J., and Ouattara, L. (2025). Electrooxidation of Oxacillin on a Boron-doped Diamond Electrode: A Voltammetric Investigation. American Journal of Applied Chemistry, 13(3), 63-72. https://doi.org/10.11648 /j.ajac.20251303.1.

[25] Koffi, K. S., Kambiré, O., Gnamba, C. Q-M., Kimou, K. J., M., Berté, Kouadio, K. E., Kone, S., and Ouattara, L. (2023) Electrochemical Detection of Paracetamol and Iohexol Using a Boron-Doped Diamond Anode Modified with Gold Particles. American Journal of Applied Chemistry, 11 (4), 103-111. https://doi.org/10.11648/j.ajac.20231104.12.

[26] Martínez-Uroz, M. A., M. Mezcua., Belmonte Valles, N., and Fernández-Alba, A. R. (2012). Determination of selected pesticides by GC with simultaneous detection by MS (NCI) and μ-ECD in fruit and vegetable matrices. Analytical and Bioanalytical Chemistry, 402, 1365–1372. https://doi.org/10.1007/s00216-011-5552-8.

[27] Yi, X., Tran, N. H., Yin, T., He, Y., and Gin, K. Y-H. (2017). Removal of selected PPCPs, EDCs, and antibiotic resistance genes in landfill leachate by a full-scale constructed wetlands system. Water Research 121: 46–60. https://doi.org/10.1016/j.watres.2017.05.008.

[28] Kouadio, K.E., Kambiré, O., Koffi, K.S., Ouattara, L. (2021) Electrochemical oxidation of paracetamol on boron-doped diamond electrode: Analytical performance and paracetamol degradation. J. Electrochem. Sci. Eng, 11 (2), 71-86. https://doi.org/10.5599/jese.932.

[29] Koffi, K. M., and Ouattara, L. (2019). Electroanalytical investigation on paracetamol on boron-doped diamond electrode by voltammetry. American Journal of Analytical Chemistry), 10, 562-578. https://doi.org/10.4236/ajac.2019.1011039.

[30] Koffi, K. M., Sadia, S. P., Kouadio, B. A., Gnamba, C. Q-M., Appia, F. T. A., Koffi, K. S., and Ouattara, L. (2023). Differential Pulse Voltammetric Simultaneous Determination of Paracetamol and Omnipaque on Boron Doped Diamond Electrode: Application to Natural Tomato, Carrot, Cucumber Juices and Wastewater. American Journal of Analytical Chemistry, 14, 434-450. https://doi.org/10.4236/ajac.2023. 1410025.

[31] Koffi, K. M., Sadia, S. P., Kouadio, K. E., Koffi, K. S., Kimou, K. J., Berté, M., Gnamba, C. Q-M., Kambiré, O., Pohan, L. A. G., and Ouattara, L. (2024). Simultaneous Differential Pulse Voltammetric Determination of Omnipaque, Paracetamol and Ceftriaxone on boron-dopped diamond electrode: Application to natural carrot, cucumber juice and wastewater. Journal of Materials and Environmental Science, 11(15), 1625-1639. https://doi.org/JMES-2024-1511110.